Relationship Between Induced Polarization Relaxation Time and Hydraulic Characteristics of Water-Bearing Sand

Zhao Ma
Shandong University
Lichao Nie (lichaonie@163.com)
Shandong University https://orcid.org/0000-0003-3177-4052
Zhaoyang Deng
Shandong University
Xin Yin
Hohai University
Junfeng Shen
Shandong University
Ningbo Li
General Institute of Water Resources and Hydropower Planning and Design

Research Article

Keywords: Induced polarization method, Darcy seepage experiment, Permeability, Relaxation time

Posted Date: November 30th, 2021

DOI: https://doi.org/10.21203/rs.3.rs-334977/v1

Relationship between induced polarization relaxation time and hydraulic characteristics of water-bearing sand

Order of Authors: *Zhao Ma[a,b], Lichao Nie[a,c,]*, Zhaoyang Deng[a,c], Xin Yin[d] , Junfeng Shen[a,c], Ningbo Li[e]*

([a]Geotechnical and Structural Engineering Research Center, Shandong University, Jinan 250061, China;
[b]School of Qilu Transportation, Shandong University, Jinan, Shandong 250061, China;
[c]School of Civil Engineering, Shandong University, Jinan, 250061, China;
[d]School of Civil and Transportation Engineering, Hohai University, Nanjing 210098, China;
[e]General Institute of Water Resources and Hydropower Planning and Design, Ministry of Water Resources, Beijing 1000120, China)

Corresponding author's full contact details:

Dr. Lichao Nie

Geotechnical and Structural Engineering Research Center, Shandong University, Jinan, 250061, China

School of Civil Engineering, Shandong University, Jinan, 250061, China

Phones: +86 18668970507(office)

E-mail: lichaonie@163.com

Information of other authors:

Zhao Ma

Geotechnical and Structural Engineering Research Center, Shandong University, Jinan, 250061, China

School of Qilu Transportation, Shandong University, Jinan, Shandong 250061, China

(mazhaofrank@163.com)

Zhaoyang Deng

Geotechnical and Structural Engineering Research Center, Shandong University, Jinan, 250061, China

School of Civil Engineering, Shandong University, Jinan, 250061, China

(1311421252@qq.com)

Xin Yin

School of Civil and Transportation Engineering, Hohai University, Nanjing 210098, China

(deric.7@foxmail.com)

Junfeng Shen

Geotechnical and Structural Engineering Research Center, Shandong University, Jinan, 250061, China

School of Civil Engineering, Shandong University, Jinan, 250061, China

(shenjunfengsd@163. com)

Ningbo Li

General Institute of Water Resources and Hydropower Planning and Design, Ministry of Water Resources, Beijing 1000120, China

(liningbo@giwp.org.cn)

Relationship between induced polarization relaxation time and hydraulic characteristics of water-bearing sand

Abstract: Induced polarization method has become a popular method for evaluating formation permeability characteristics in recent years because of its sensitivity to water body and water-bearing pore structure. Especially, the induced polarization relaxation time can reflect the macroscopic characteristics of the pore structure of rock and soil. Therefore, in order to study the relationship between relaxation time and permeability, eight different sizes of quartz sand were used to simulate water-bearing sand layers under different working conditions, and the induced polarization experiment and Darcy seepage experiment were carried out on the same sand sample in this paper, respectively. The experimental results show that the relation time and the evolution of the permeability are closely correlated with the sizes of quartz sand. According to the experimental data, with the particle size of the quartz sand as the link, the power function equation is fitted to better describe the relationship between the permeability and the relation time. It is worth noting that the equations obtained are only empirical equations for quartz sand and are not suitable for general applications.

Keywords: Induced polarization method; Darcy seepage experiment; Permeability; Relaxation time

1. Introduction

With the increase of number of deep and long tunnels, disaster-causing water-bearing structures have caused water and mud bursts in front of tunnels, it has become an important problem in some tunnels. The water permeability of the water-bearing structure, that is, the permeability characteristics, directly determines the magnitude and scale of water inrush. It is essential to estimate the magnitude and scale of water inrush with proper evaluation of the permeability characteristics of water-bearing structures (Ni et al., 2010). In general, laboratory measurement of borehole sampling, field experiment methods such as pumping experiment or pressure experiment are being used to understand the permeability characteristics of water-bearing structures in front of tunnel face (Attwa et al., 2013). However, these methods are expensive and due to the limitation of the number of samples and ex-situ experiment s, their results often have hysteresis and one-sidedness. The induced polarization method has the advantage of being sensitive to the pore structure of the formation and not being affected by topographical factors, and

it is more and more used to predict the hydraulic characteristics of the formation (Slater, 2007).

The induced polarization method is a geophysical method based on the induced polarization effect of the geological body, which is based on the difference of induced polarization parameters between different rock and soil media. Observing the complex conductivity and polarizability of the rock-soil medium, we can get information such as the real part characterizing the charge conduction characteristics and the imaginary part characterizing the charge storage characteristics in the complex conductivity. Permeability determines the resistance of porous materials to fluid flow (Lesmes et al., 2001; Revil et al., 2010). In the detection of disaster-causing water-bearing structures in tunnels, the fluid is usually groundwater and its properties are relatively stable. Therefore, the permeability (k) can be used to evaluate the permeability of the formation. In 1957, the induced polarization method was first proved to be applicable to groundwater detection, and pointed out that the permeability of shallow aquifers can be evaluated by the relevant parameters of the induced polarization attenuation curve (Vacquier et al., 1957). In the past ten years or so, more and more articles have shown that the imaginary component of the complex conductivity of rock and soil is positively correlated with the specific surface area of the medium. Combined with the Kozeny-Carman formula, the relationship between permeability, porosity and specific surface area can be obtained (Borner et al., 1991; Schon, 2015; Slater L et al., 2002; Slater L et al., 2006). However, some scholars found that the correlation between the imaginary part of the complex conductivity and the specific surface area is weak when using British sandstone for experiments, and it is difficult to meet the accuracy requirements for predicting permeability (Binley et al., 2005). The above method essentially uses indirect parameters such as porosity and specific surface area to evaluate permeability, and the estimation results have certain instabilities.

Previous studies have shown that permeability calculations can be carried out by using the correlation between relaxation time and pore size, and the calculated results are in good agreement with the directly measured permeability (Niu et al., 2016). However, some scholars have proposed that the permeability calculation method based on the relationship between relaxation time and pore size has certain limitations, and it is difficult to obtain a universally applicable prediction model for mixed particle size samples (Joseph et al., 2016; Kruschwitzv et al., 2010; Titov et al., 2010). The relaxation time spectrum inversion method is to obtain the excitation polarization relaxation time distribution of the sample from the time-domain attenuation curve, and use the excitation polarization relaxation time

spectrum to characterize the pore structure distribution and estimate the permeability (Tong et al., 2006a; Tong et al., 2006b; Titov et al., 2010). In addition, some scholars have studied the relationship between the two in terms of models, using the average relaxation time (τ) of the complex resistivity Cole-Cole model to estimate the permeability of sandstone. Revil and Florsch proposed a model showing that permeability is linearly related to relaxation time (Binley et al., 2005; Revil et al., 2010). The above method research shows to varying degrees that there is a correlation between relaxation time and permeability.

In this paper, 8 kinds of quartz sands are used to simulate the water-bearing sand layer under different working conditions, and the indoor and outdoor experiments are carried out through the designed multiple experiment devices. The first is the induced polarization experiment, which uses square experiment tanks of different sizes to fill quartz sand samples of different particle sizes to obtain the observation data of the induced polarization experiment, and then obtain the relaxation time. The second is the measurement of permeability. Using the same sample, the Darcy percolation experiment is performed to determine the permeability parameters to obtain the permeability. Considering the particle size of the water-bearing sand sample as the intermediate quantity, the relationship between relaxation time and permeability is established through the compound mapping relationship of relaxation time-sand sample size-permeability. The relationship between the two will be further clarified to verify the effectiveness of the method for estimating the induced polarization permeability.

2. Experimental Principles and Method

2.1 Quartz sand sample preparation

In order to simulate different pore structures of various formations, at the same time, considering the ease of control and preparation of loose samples, quartz sand is used as the formation simulation material. Fine quartz sand is selected, in order to ensure the differentiation of particle size, this experiment uses custom-made screens with different apertures to screen the quartz sand. The quartz sand is divided into 8 particle sizes: 0.1~0.2mm, 0.2~0.5mm, 0.5~1mm, 1~2mm, 2~3mm, 3~4mm, 4~6mm, 6~8mm.

The sieved quartz sand still has some impurities. In order to avoid clay or other impurities having a significant impact on the induced polarization effect, the sieved sand sample is cleaned, dried, and then

poured with water to saturation for testing. The water sample used was the site water of the tunnel project to simulate the actual engineering conditions. The quartz sand after screening and cleaning is shown in Fig.1. At the same time, in order to reduce the influence of temperature on the induced polarization effect, the measurement needs to be carried out in an environment with small temperature changes.

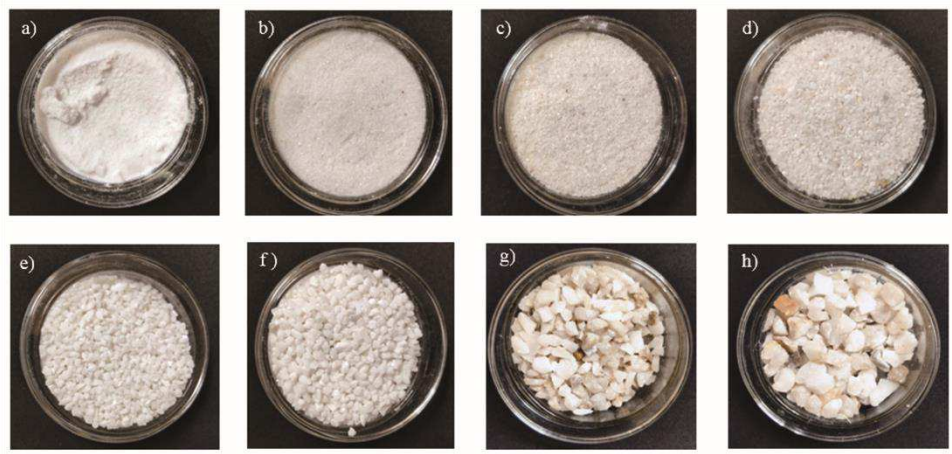

Fig. 1 sand of samples with different particle size grades. a) 0.1-0.2 mm, b) 0.2-0.5 mm, c) 0.5-1 mm, d) 1-2 mm, e) 2-3 mm, f) 3-4 mm, g) 4-6 mm, h) 6-8 mm

2.2 Induced polarization experiment

The commonly used detection methods of the induced polarization method are time domain and frequency domain. Time domain measurement has the advantages of high efficiency and convenient operation in the field work. Through the measurement of a charge and discharge process, all time domain induced polarization observation data can be obtained, which can greatly save field work time and may reduce work efficiency. Therefore, the time-domain measurement method is used for the experimental study of induced polarization. In the observation device of the experiment, four-electrode arrangement is used for measurement. The outer side is two current electrodes. In order to reduce the influence of the polarization of the current electrodes and the potential electrodes on the measurement results, the current electrode A/B uses graphite electrodes, as shown in Fig. 2(a). There are two potential electrodes on the inner side. In order to avoid the influence of the polarization of the electrodes on the observation data, there are two potential electrodes M/N on the inner side, using Ag/Agcl non-polarized electrodes, as shown in Fig. 2(b). The electrolyte adopts saturated KCL solution and is replaced regularly. The purpose is to prevent the electrolyte from failing due to long-term use, resulting in the generation of over-potential of the electrode itself, and to minimize the influence of the polarization of the electrode on the

measurement result.

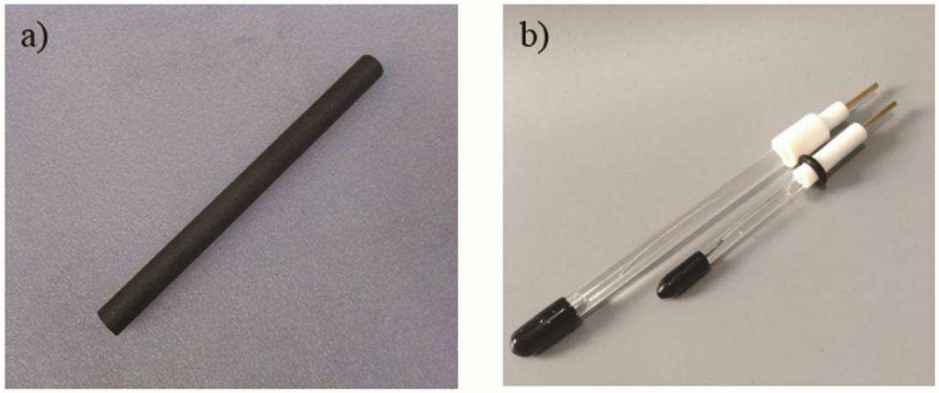

Fig. 2 The current electrode and potential electrode. a) Graphite current electrode, b) Ag/AgCl unpolarized potential electrode

The experiment transmitter uses Pentium WDFZ-10T excited polarization transmitter. The signal transmitter is connected to the current electrode, which can transmit DC square wave signals with different duty ratios and different power supply durations, and can measure the current size of the transmitted signal. The receiver adopts Horn3D full-function IP instrument, its sampling frequency is up to 250Hz, and it can collect full waveform time series data.

The used transmission period and reception period are both 64s. In order to eliminate the influence of DC offset caused by unidirectional power supply, each cycle uses square wave pulses of opposite polarity to supply power with a duty cycle of 50%, that is, the power supply duration is the same as the power failure duration. At the same time, in order to reduce accidental errors in the data process, multiple cycles of power supply and power failure measurements were performed, so the power supply current signal of the transmitter is shown in Fig. 3(a).

In terms of data collection, the receiver adopts a late synchronization method for data collection, without manual synchronization of the transmitted signal. The obtained observation signal is shown in Fig. 3(b). It can be seen that the secondary field voltage slowly decays within a certain period of time after the power supply signal is turned off.

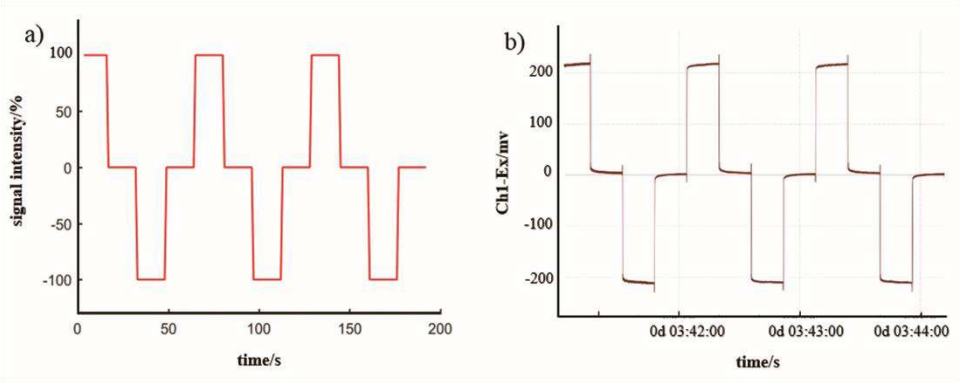

Fig. 3 a) Schematic of current signal, b) Measured full waveform signal

We try a larger outdoor square experiment tank with a size of 100cm×100cm×100cm is used, as shown in Fig. 4. The side walls and the ground are made of cement. Data collection is performed on the process of excited polarization power supply and power-off, and time-domain attenuation information is obtained.

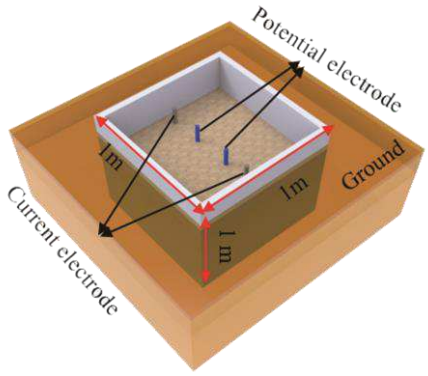

Fig. 4 Outdoor laboratory tank

2.3 Darcy flow experiment

In order to experiment the actual permeability coefficient of the quartz sand samples and calculate the permeability, the Darcy seepage experiment device was used to conduct seepage experiments on quartz sand samples with different particle sizes. Since the sample is highly water-permeable, the measurement is carried out by the constant head method. The experimental instrument is shown in Fig.5; the current experiment system is mainly comprised of five parts:

(1) Water supply device: it can realize continuous replenishment of experimental water and keep the water head stable during the experiment;

(2) Permeation device: an acrylic cylinder is used to place the experiment sample, the upper end is

equipped with a water inlet, the side is equipped with a pressure measuring hole, the lower end is equipped with a water outlet, and the bottom is equipped with a permeable filter plate;

(3) Pressure measuring device: connect the pressure measuring tube with the pressure measuring hole to measure the pressure head on different sections;

(4) Drainage device: set a series of round holes in the piezometric tube to adjust the drainage water level;

(5) Other equipment: stopwatch, 1000mL measuring cylinder, beaker, funnel, glass rod, thermometer, tube clamp, rubber tube and suction balloon, etc.

Fig. 5 Schematic diagram of Darcy seepage tester

Before the formal experiment, first determine the relationship between the permeability of the quartz sand sample and the head loss, and test the experimental instrument. After confirming that the experimental instrument is in good condition, the permeability measurement of 8 kinds of homogeneous quartz sand samples with particle size is carried out. The experimental process is as follows:

(1) Connect the instrument: check the state of the instrument, such as whether the piezometer tube and the infiltration device are airtight, and record the inner diameter of the infiltration device, the distance between the piezometer tubes and other parameters;

(2) Filling the sample: first install a permeable filter plate at the bottom of the infiltration device, then the sample is loaded, every time a certain thickness is loaded, a certain degree of vibrating is performed with a glass rod;

(3) Saturated sample: inject water from top to bottom until water film appears on the surface of the sample;

According to Darcy's law, the seepage flow Q of the cross section through the infiltration device is

proportional to the cylindrical section A and the hydraulic slope I, and is related to the soil permeability coefficient K. The basic relationship is as follows:

$$Q = KAI \tag{1}$$

$$I = (H_2 - H_1) / L \tag{2}$$

Where I is the hydraulic gradient, H_1 and H_2 are respectively the head of the piezometer, and L is the length of the seepage path, both in m.

(4) Experimental measurement: After the water level of the piezometric pipe is stable, record the piezometric water level and start to measure the seepage flow out of the permeation device within a certain period of time. After repeating the measurement, change the hydraulic slope of the device and repeat the above process for measurement. In order to prevent the osmotic pressure in the device from changing too drastically and damaging the original structure of the sample, the hydraulic gradient should be increased or decreased step by step to avoid jumping changes.

The permeability coefficient K can be used to evaluate the difficulty of the fluid passing through the pore framework of rock and soil, and its definition is shown in Eq. (3):

$$K = k \frac{\rho g}{\mu} \tag{3}$$

Where ρ is the fluid density, g is the acceleration due to gravity, and μ is the hydrodynamic viscosity coefficient.

The Darcy seepage experiment is used to test samples of different particle sizes. According to the above operation method, the flow rate is changed 2 to 3 times to obtain the flow rate, time, head and other parameters, and the permeability coefficient and permeability are calculated by Eq. (3). Record and analyze the experiment data.

3. Results and discussions

3.1 Relaxation time measurements

In order to verify the repeatability of the experimental data and reduce the impact of accidental errors on the measurement results, the same measurement device is used to perform repeated observations on the same sample. In the time domain induced polarization experiment, the attenuation curve of the secondary field at the corresponding particle size is obtained, and the attenuation curve of the polarization

rate is obtained by Eq. (4).

$$\eta_s = \frac{\Delta U_2(t)}{\Delta U(T)} \tag{4}$$

Where η_s is polarization rate , $\Delta U(T)$ is the total field potential difference measured before the power is cut off by supplying power to the body polarized medium with a stable current for a period of time *T*, $\Delta U_2(t)$ is the secondary field potential difference measured at time *t* after power failure.

We obtain the polarizability decay curve of the corresponding particle size under a certain current from the average of multiple sets of data, and fit it with the second nonlinearity of the Cole-Cole model to obtain the relaxation time curve under the corresponding particle size. Table 1 shows the relaxation time distribution of different particle sizes.

Table 1 Relaxation time of sand sample

Particle size (mm)	0.1~0.2	0.2~0.5	0.5~1	1~2	2~3	3~4	4~6	6~8
The relaxation time (s)	0.410	0.541	0.857	1.035	1.273	1.552	1.705	2.215

The relaxation time curves of eight different particle sizes of quartz sand are shown in Fig.6.

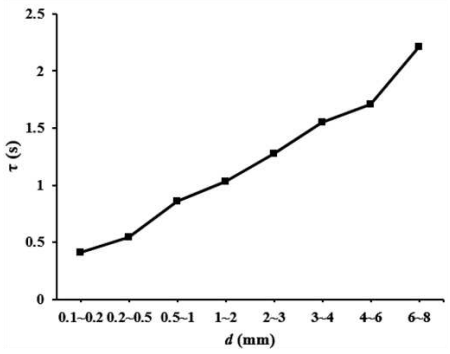

Fig. 6 Relaxation time of sand sample

3.2 Permeability measurements

Through measurement, the inner diameter of the instrument *D*=6.4cm, the cross-sectional area of the quartz sand sample *A*=0.0033m^2, and the pressure measurement interval *L*=10cm. The outdoor temperature was continuously measured for three days, and the average temperature for three days was 15°C, so the hydrodynamic viscosity coefficient was 0.001*Pa·s*. Use the constant head method to test. After the water flow remains stable, record the experiment data when the water flow out of the drain is

1000mL. The permeability coefficient of the sample can be calculated through the measurement results of the Darcy seepage experiment, and the permeability of the quartz sand sample of this particle size can be obtained by conversion by Eq. (3). The experimental data is shown in the following table 2:

Table 2 Darcy experiment result

Particle size (mm)	Time t(s)	Water volume $w(m^3)$	Flow $Q(m^3/s)$	Piezometer water level (cm)		Water level difference (cm)	Hydraulic gradient I	Permeability coefficient K(m/s)	Permeability $k(m^2)$
				h_1	h_2	h_1-h_2			
0.1~0.2	189	0.001	5.3E-06	20	2	18	1.8	9.1E-04	9.1E-11
0.2~0.5	92.6	0.001	1.1E-05	20	2	18	1.8	1.9E-03	1.9E-10
0.5~1	66.3	0.001	1.5E-05	20	2	18	1.8	2.6E-03	2.6E-10
1~2	62	0.001	1.6E-05	20	2	18	1.8	2.8E-03	2.8E-10
2~3	61.5	0.001	1.6E-05	20	2	18	1.8	2.8E-03	2.8E-10
3~4	22	0.001	4.5E-05	20	2	18	1.8	7.9E-03	7.9E-10
4~6	20.6	0.001	4.9E-05	20	2	18	1.8	8.4E-03	8.4E-10
6~8	14.3	0.001	7.0E-05	20	2	18	1.8	1.2E-02	1.2E-09

It can be seen that as the particle size of the quartz sand sample increases, the time required to reach the same seepage flow has a significant difference, and the difference between the minimum and maximum time is close to 10 times. Through data such as flow, time, pressure head, etc., through data such as flow, time and pressure head, it is possible to calculate parameters such as seepage flow, seepage velocity, water level difference and hydraulic slope, so as to obtain permeability coefficient and permeability from Darcy's law. The experimental results show that the evolution of the permeability is closely correlated with the sizes of sand sample.

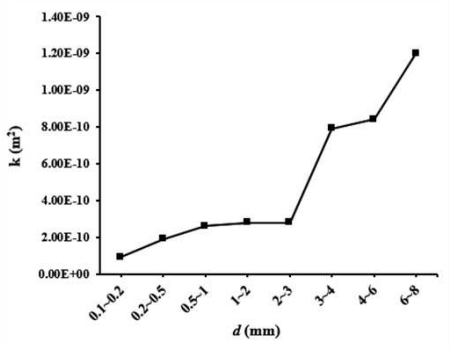

Fig. 7 Permeability of sand sample

3.3 Fitting of curves

According to the experimental data, the power function equation is used to fit the relaxation time and permeability of the same particle size sand sample, and the empirical equations for the relationship

between the permeability and the relaxation time is obtained, and the relationship between relaxation time and permeability is established. The fitting equations are given below.

$$k = 0.003\tau^{1.4315} \quad (5)$$

The relationship between relaxation time and permeability under the same particle size is shown in the fig. 8 below:

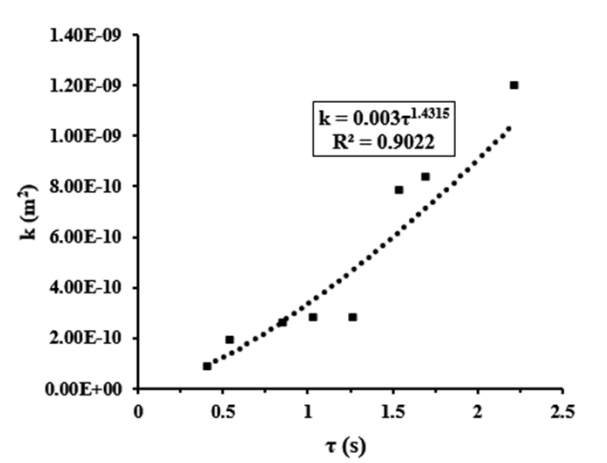

Fig. 8 Relationship between relaxation time and permeability

4. Conclusion

In this paper, 8 kinds of quartz sands with different particle sizes are used to measure the relaxation time and permeability of sand samples with different particle sizes using the field time domain induced polarization experiment system and the indoor Darcy flow experiment system. According to the experimental data, the following conclusions can be made:

(1) The relaxation time and permeability increase with the increase of quartz sand particle size, and the increasing trend gradually increases, which has a significant positive correlation.

(2) Using the particle size of the water-containing sand sample as the intermediate quantity, the relationship curve of permeability and relaxation time under the same particle size is formed by mathematical fitting. Finally, the power function equation to describe the correlation between relaxation time and permeability is obtained.

In this paper, the obtained relationship is the experiment equation of quartz sands. They are not for the universal equations application, and their coefficients may be different in different experiment conditions and rock samples.

Reference

295 Ni X, Wang Y, Lu Y (2010) Study of meso-mechanism of seepage failure in tunnel excavation process.
296 Chin J Rock Mech Eng 29(4):194-4
297 Attwa M, Günther T (2013) Spectral induced polarization measurements for predicting the hydraulic
298 conductivity in sandy aquifers. Hydrol Earth Syst Sc 17(10):4079-4094. https://doi.org/
299 10.5194/hess-17-4079-2013.
300 Slater L (2007) Near surface electrical characterization of hydraulic conductivity: From petrophysical
301 properties to aquifer geometries—A review. Surv Geophys 28(2-3):169-197. https://doi.org/
302 10.1007/s10712-007-9022-y.
303 Lesmes D P, Frye K M (2001) Influence of pore fluid chemistry on the complex conductivity and induced
304 polarization responses of Berea sandstone. J Geophys Res-Sol Ea 106(B3):4079-4090.
305 https://doi.org/ 10.1029/2000JB900392
306 Revil A, Florsch N (2010) Determination of permeability from spectral induced polarization in granular
307 media. Geophys J Int (3):1480-1498.https://doi.org/10.1111/j.1365-246X.2010.04573.x
308 Vacquier V, Holmes C R, Kintzinger P R Lavergne M (1957) Prospecting for Ground Water by Induced
309 Electrical Polarization. Geophysics 22(3): 660. https://doi.org/10.1190/1.1438402
310 Borner F, Schopper J, Weller A (1996) Evaluation of transport and storage properties in the soil and
311 groundwater zone from induced polarization measurements1. Geophys Prospect 44(4): 583-601.
312 https://doi.org/10.1111/j.1365-2478.1996.tb00167.x
313 Schon J H (1997) Physical properties of rocks: Fundamentals and principles of petrophysics. Seismic
314 Exploration. https://doi.org/10.1029/97EO00363
315 Slater L, Lesmes D P (2002) Electrical-hydraulic relationships observed for unconsolidated sediments.
316 Water Resour Res 38(10): 31-31-31-13. https://doi.org/10.1029/2001WR001075
317 Slater L, Ntarlagiannis D, Wishart D (2006) On the relationship between induced polarization and surface
318 area in metal-sand and clay-sand mixtures. Geophysics 71(2): A1-A5.
319 https://doi.org/10.1190/1.2187707
320 Binley A, Slater L, Fukes M, et al (2005) The relationship between frequency dependent electrical
321 conductivity and hydraulic properties of saturated and unsaturated sandstone. Water Resour Res
322 41(12): W12417.
323 Niu Q, Revil A (2016) Connecting complex conductivity spectra to mercury porosimetry of sedimentary
324 rocks. Geophysics 81(1): E17-E32. https://doi.org/10.1190/geo2015-0072.1

Joseph S, Ingham M, Gouws G (2016) Spectral-induced polarization measurements on sieved sands and the relationship to permeability. Water Resour Res 52(6). https://doi.org/4226-4246. 10.1002/2015WR018087

Kruschwitz S, Binley A, Lesmes D Elshenawy A (2010) Textural controls on low-frequency electrical spectra of porous media. Geophysics 2010, 75(4): WA113-WA123. https://doi.org/10.1190/1.3479835

Titov K, Tarasov A, Ilyin Y Seleznev N (2010) Relationships between induced polarization relaxation time and hydraulic properties of sandstone. Geophys J Int 180(3): 1095-1106. https://doi.org/10.1111/j.1365-246X.2009.04465.x

Tong MS, Li L, Wang WN Jiang YZ (2006) Determining capillary-pressure curve, pore-size distribution, and permeability from induced polarization of shaley sand. Geophysics 71(3): N33-N40. https://doi.org/10.1190/1.2195989

Tong MS, Li L, Wang WN, Jiang YZ (2006) A time-domain induced-polarization method for estimating permeability in a shaly sand reservoir. Geophys Prospect 54(5): 623-631. 10.1111/j.1365- https://doi.org/2478.2006.00568.x